

Supplementary information

Electrochemical synthesis of metal and semimetal nanotube-nanowire heterojunctions and their electronic transport properties

Dachi Yang,^{ab} Guowen Meng,^{*a} Shuyuan Zhang,^c Yufeng Hao,^{ab} Xiaohong An,^{ab}

Qing Wei,^{ab} Min Ye^{ab} and Lide Zhang^a

^aKey Laboratory of Materials Physics, and Anhui Key Laboratory of Nanomaterials and Nanostructures, Institute of Solid State Physics, Chinese Academy of Sciences, Hefei, 230031 China. E-mail: gwmeng@issp.ac.cn; Fax: (86)551-5591434

^bGraduate School of Chinese Academy of Sciences, Beijing, 100039, People's Republic of China

^cStructure Research Lab, University of Science and Technology of China, Hefei, 230026 China.

Table of Contents:

1. Experimental details.
2. Electrochemical synthesis of BiNT-CuNW heterojunction.
3. The controlling crystallization of the BiNT-CuNW heterojunctions.
4. HRTEM image of BiNT-CuNW junction.

1. Experimental details

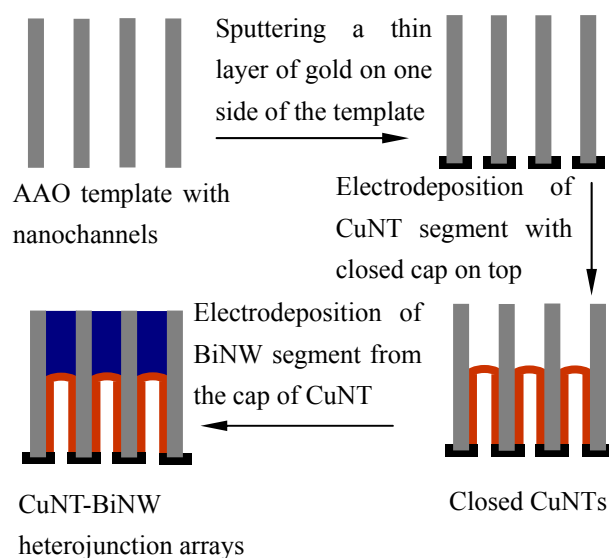


Figure 1. Schematic illustration of synthesizing CuNT-BiNW heterojunction arrays.

Preparation of AAO template and sputtering gold layer:

The AAO templates were fabricated via a two-step anodization process in 0.3M oxalic acid solution under 40V_{DC}.^{1,2} Then the above AAO templates were put in a 5wt% H₃PO₄ solution at 40 °C for 35 min to remove the barrier layer and widen the nanochannels. The final through-hole AAO templates are about 60 μm in thickness with nanochannels about 80 nm in diameter. A thin gold layer was sputtered on one side of the AAO template to serve as working electrode during the electrochemical deposition. It should be mentioned that the gold layer should be thin enough to leave the pores open and cover only the top-view surface of the pore walls, which can be achieved by adjusting the sputtering parameters.

Electrochemical Deposition of CuNT-BiNW heterojunction arrays:

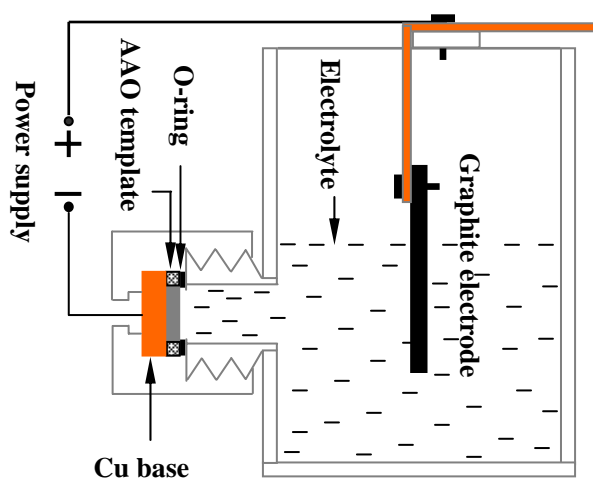


Figure 2. The electrochemical deposition set-up

For the confined electrochemical deposition inside the nanochannels of the anodic aluminium oxide (AAO) template, a specially constructed electrochemical cell was used (Figure 2). The cell consists of a cylindrical copper base onto which the Au-coated AAO template was placed with the Au layer facing the Cu base, which was screwed onto a polymethyl methacrylate (PMMA) cell, with a rubber O-ring in between to seal them up. The electrolyte was confined to the bare side of the

template so that the electrochemical deposition would initiate onto the thin Au layer at the template bottom and continue outward from the pore bottom to the pore opening.

The electrolyte we used for CuNTs and CuNWs contains 0.2M $\text{CuSO}_4 \cdot 5\text{H}_2\text{O}$ and 0.1M H_3BO_3 ,³ which was buffered to $\text{pH} = 4.5 \sim 5.0$ with H_2SO_4 solution. The electrolyte for BiNWs and BiNTs contains 75g/l $\text{Bi}(\text{NO}_3)_3 \cdot 5\text{H}_2\text{O}$, 125g/l $\text{C}_3\text{H}_5(\text{OH})_3$, 50g/l $\text{C}_4\text{H}_6\text{O}_6$, and 65g/l KOH,⁴ which was buffered to $\text{pH} = 0.9$ with nitric acid. For CuNT-BiNW heterojunction arrays, the Au-coated AAO template was mounted on the PMMA cell, CuNTs segments were electrodeposited inside the half depth of the nanochannels under a constant current density of 2.2 mA/cm^2 for 30 min at room temperature, with a graphite plate as the counter electrode. After the power supply was suddenly switched off, the Cu electrolyte was emptied out from the cell. The AAO template with electrodeposited CuNTs segments was rinsed with deionized water, and mounted on the PMMA cell again. Then, BiNWs segments were electrodeposited inside the remaining half depth of the nanochannels on the closed caps of CuNTs at a constant current density of 2.2 mA/cm^2 for 30 min.

Structural Characterization of CuNT-BiNW heterojunctions: In order to release the electrodeposited heterojunctions from the AAO template, the AAO templates were dissolved with a 5% NaOH solution, rinsed in deionized water thoroughly, and then characterized by using field-emission scanning electron microscope (FE-SEM, Sirion 200, at 5kv) with energy dispersive X-ray spectroscopy (EDS, OXFORD), transmission electron microscopy (TEM, Hitachi 800, at 200kv) and high resolution TEM (HRTEM, JEOL-2010, at 200kv).

I-V Curve Measurements of CuNT-BiNW and BiNT-CuNW heterojunction: DC four-probe method was used in the I-V curve measurements. Before the measurements, a gold layer was sputtered on the dual sides of the samples as conducting electrodes. Colloidal silver was used to connect copper wires with the gold layer on AAO template. Then the current of CuNT-BiNW

heterojunction arrays and BiNT-CuNWs heterojunction arrays was controlled in the range of $-1 \sim 1$ mA and $-50 \sim 50$ mA, respectively.

2. Electrochemical synthesis of BiNT-CuNW heterojunction

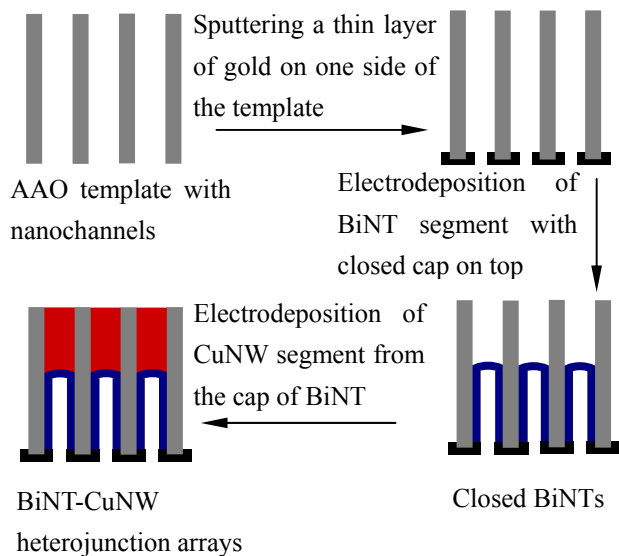


Figure 3. Schematic illustration of synthesizing BiNT-CuNW heterojunction arrays.

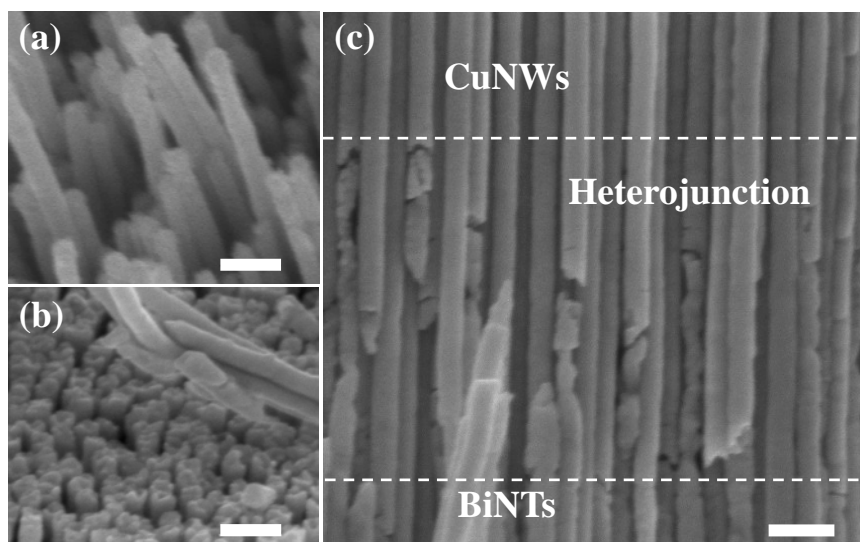


Figure 4. (a) Top view SEM image of CuNWs. (b) Bottom view SEM image of BiNTs. (c) Side view SEM image of BiNT-CuNW heterojunction arrays. The scale bars are all 200nm.

Similar to CuNT-BiNW heterojunction arrays, if the electrodeposition sequence is changed,

BiNT-CuNW heterojunction arrays can be obtained. Fig.3 schematically illustrates the synthesizing process. Firstly, BiNT segments were electrodeposited inside the half depth of the nanochannels under a constant current density of 2 mA/cm² for 30 min at room temperature. After the power supply was suddenly switched off, the Bi electrolyte was emptied out from the cell. Then, CuNW segments were electrodeposited inside the remaining half depth of the nanochannels on the closed caps of BiNTs at a constant current density of 2.2 mA /cm² for 30 min. Fig.4a and Fig.4b are the top-view SEM images of the CuNWs and bottom-view of the BiNTs, respectively. Fig.4c is the side-view SEM image of BiNT-CuNW heterojunction arrays, and the area where the junctions are located is in between the two dashed lines.

3. The controlling crystallization of the BiNT-CuNW heterojunction:

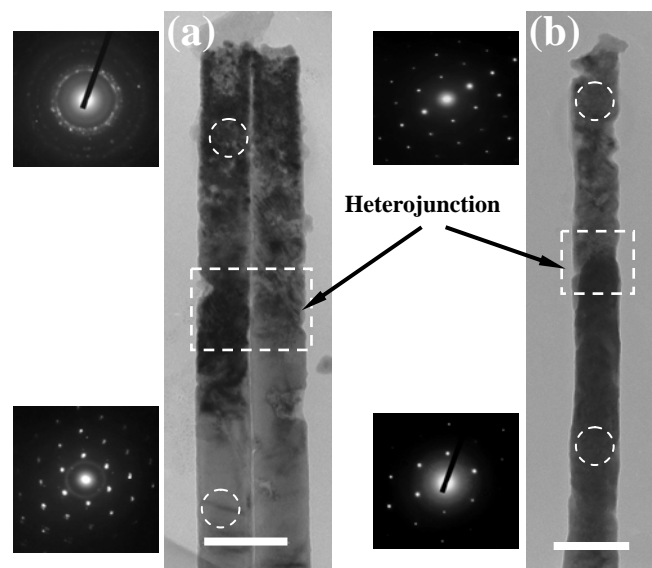


Figure 5. BiNT-CuNW heterojunctions. (a) Bi NT is polycrystalline, while Cu NW is single crystalline. (b) Both Bi NT and Cu NW are single-crystalline. The scale bars are all 100nm.

We have tried many experiments by using the same AAO templates coated gold layers with different thickness, and then found that the crystallization of NT-NW can be controlled. Herein, we

take BiNT-CuNW heterojunctions as an example, under the proper electrodepositing conditions, when relatively thinner gold layer was coated on the template, we can obtain BiNT-CuNW heterojunctions (Fig.5a) with the thinner NT being polycrystalline and the NW being single-crystalline, respectively. In contrast, when relatively thick gold layer was coated on the template, the NT wall is much thicker, and both the NT and NW are single-crystalline (Fig.5b).

4. HRTEM image of BiNT-CuNW heterojunction.

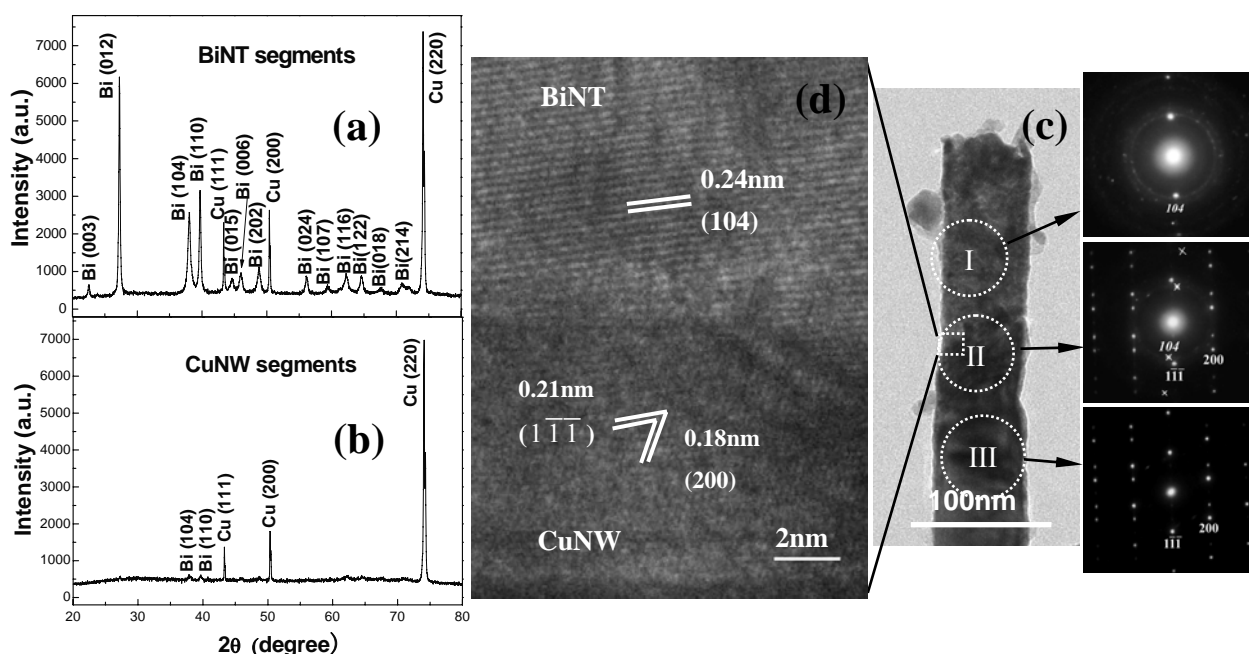


Figure 6. (a), (b) XRD patterns taken from the BiNT and CuNW segments, respectively. (c) TEM image of BiNT-CuNW Heterojunction with corresponding SAED patterns (the SAED pattern in the junction region, the spots of Bi are marked by “×”). (d) HRTEM image of heterojunction taken from the dashed rectangle of (c).

The HRTEM and XRD characterizations give further structural features of NT-NW heterojunctions. Fig.6a and 6b show the XRD spectra taken from the BiNT segment side and the CuNW segment side, respectively. In our experiments, we synthesized the BiNT-CuNW heterojunction with BiNT segment about 300nm (Fig. 6c) and CuNW segment about 20 μ m in length, respectively. So there still appears strong Cu peak in the XRD spectrum taken from the BiNTs segment side. In contrast, there appears relatively weak Bi peak in XRD spectrum taken from the CuNWs segment side. Besides, the SAED

patterns in Fig. 6c show that BiNTs and CuNWs are polycrystalline and single-crystalline, respectively. The lattice-resolved image taken from the heterojunction region of BiNT-CuNW (the dashed rectangle in the Fig. 6c) shows that the lattice spacing of BiNT and CuNW are about 0.24nm (rhombus-structured Bi(104) planes) and 0.21nm (face-centered Cu ($1\bar{1}\bar{1}$) planes). With the SAED pattern, it can be seen that the BiNT and the CuNW are close to grow along (104) planes and $[1\bar{1}\bar{1}]$ direction, and that zone axis of CuNT is [011] direction. From the lattice-resolved image and the SAED at the junction region, the Bi(104) planes are approximately parallel to Cu ($1\bar{1}\bar{1}$) planes. However, we can find that it still has a little angle about 2° between Bi(104) (marked “×”) and Cu (111) plane. As a result, it is difficult to judge what the relation is between the two planes at the interfacial region.

Notes and references

- 1 G. W. Meng, A. Y. Cao, J. -Y. Cheng, A. Vijayaraghavan, Y. J. Jung, M. Shima and P. M. Ajayan, *J. Appl. Phys.* 2005, **97**, 064303.
- 2 F. H. Xue, G. T. Fei, B. Wu, P. Cui, and L. D. Zhang, *J. Am. Chem. Soc.* 2005, **127**, 15348.
- 3 T. Gao, G. W. Meng, Y. W. Wang, S. H. Sun and L. D. Zhang, *J. Phys.: Condens. Matter.* 2002, **14**, 355.
- 4 Y. T. Tian, G. W. Meng, S. K. Biswas, P. M. Ajayan, S. H. Sun, and L. D. Zhang, *Appl. Phys. Lett.* 2004, **85**, 967.